Online at: https://researchtrendsjournal.com
Indexed Journal

ISSN No: 2584-282X
Peer Reviewed Journal

INTERNATIONAL JOURNAL OF TRENDS IN EMERGING RESEARCH AND DEVELOPMENT

Volume 3; Issue 4; 2025; Page No. 114-123

Received: 01-04-2025
Accepted: 13-05-2025

Flexural deformation behaviour of two-way slabs reinforced with African fan palm bars (AFP) of varying tensile strengths

[1]Edward C Mansal, [2]Charles K Kankam, [3]Vincent Akortia, [2]Russel O Afrifa, [2]Jack O Banahene, [2]Selase AK Kpo, [4]Theophilus Kwaako and [2]Enock Tongyem

[1]College of Engineering: The University of Applied Science, Engineering and Technology (USET), Brikama, The Gambia, West Africa
[2]Department of Civil Engineering, Kwame Nkrumah University of Science and Technology (KNUST), Kumasi, Ghana
[3]Department of Civil Engineering, Ho Technical University, Ho, Ghana
[4]University of Ghana, PDMSD, Legon, Ghana

DOI: https://doi.org/10.5281/zenodo.16813230

Corresponding Author: Edward C Mansal

Abstract

This experimental study investigated the flexural strength and deformation of fan palm reinforced two-way concrete slabs subjected to concentrated central load. With increasing interest in sustainable and low-cost construction materials, particularly in developing countries, the use of the African fan palm (AFP) offers a promising solution. Known for its tensile strength and durability, the AFP is widely used in structural construction such as roof works. In this study, a total of 12 concrete slabs reinforced with varying percentages of AFP ratios and 2 slabs with steel reinforcement were cast. Out of the 14 slabs, 12 were tested monotonically and 2 subjected to cyclic loading. The mid-span deflection, crack pattern, ultimate load capacity and failure modes of the slabs were recorded and evaluated. Results indicated that the ratio of the average experimental failure loads (P_{ult}) to theoretical failure loads (P'_{ult}) of all fan palm reinforced slabs TWS1-TWS6 and TWS8 - TWS13 ranged from 1.46 to 1.31 compared to the steel reinforced slabs that varied from 1.47 to 1.36. This is a good indicator of the margin of safety exhibited by the fan palm and steel bars respectively. The fan palm reinforced slabs exhibited lower ultimate load carrying capacity than the steel-reinforced slabs. Furthermore, additional load capacity was observed with increase tensile ratio of fan palm. Hence, this study proposes an ideal limit of tensile ratios for an under-reinforced fan palm concrete slab section based on IS 456:2000.

Keywords: Flexural strength, concentrated loads, monotonic loading, cyclic loading, tensile ratio

1. Introduction

With the increasing interest in sustainable and low-cost construction materials, particularly in developing countries, natural reinforcing material such as jute (Parveen and Sharma, 2013) [32], bamboo (Kankam *et al*., 1988; Adom-Asamoah *et al*., 2017 and Kumar *et al*., 2021) [25, 3, 27], raffia palm (Kankam, 1997) [22] and the African fan palm (Audu and Raheem, 2017) [10] offer promising solutions. Particular attention is now directed to natural woody materials such as bamboo, rattan, babadua and the African fan palm. The African fan palm is a single trunk mart tree with towering heights ranging from 15-25 meters or more, when fully matured. The woody mart plant is mostly found in semi-arid and sub-humid zones of Sub-Saharan Africa (ICRAF, 1992; Ayarkwa, 2007) [18, 11]. Gbesso *et al*., (2016) [17] and Michon *et al*. (2018) [30] presented various multi-functional uses of the mart tree ranging from the crown (branches) for roofing and basketry, trunk for structural timber and roots for nutrients. However, Agyarko *et al*. (2014) [4] and Michon *et al*. (2018) [30] enumerated activities such as bush fires, indiscriminate felling and overexploitation such as agricultural and excessive fruit harvesting activities as threats to the extinction of the mart tree. The authors offered solutions for the regeneration of the plant through the enactment of bye-laws and creation of *Borassus aethiopum* forest parks as means of preservation.

Empirical Studies reported significant progress undertaken on investigating both the physical properties (namely, closely dense and durable fibers, offering resistance to decay, corrosion or fungal attack when in contact with water) (Joshua, 1997) [21] and mechanical properties of fan palm such as flexural bending, modulus of rupture, compression and modulus of elasticity (Samah *et al*., 2015; Asafu-Adjaye Osei Asibe *et al*., 2013; Sohounhloue *et al*., 2018; Adedeji, 2020; Kone *et al*., 2021) [33, 7, 34, 1, 26]. Audu and Raheem (2017) [10] and Audu and Oseni (2015) [9] investigated the crack parameters and patterns in concrete slabs reinforced with fan palm subjected to sustained loads. The authors observed lower theoretical yield loads to experimental yield loads ratios. Their findings indicated good design for serviceability limit state. Furthermore, they reported that increased applied loads led increased number of cracks. Pam *et al*. (2001) [31] addressed the issue of tensile strength of fan palm and noted that lower tensile value of reinforcement provides better warning with signs of ductility compared to higher tensile values which cause the concrete to crush without yielding. Fan palm bars possess relatively good tensile strength. However, they exhibit a linearly elastic behaviour similar to the GFRP bar with a lower modulus of elasticity when compared to steel reinforcements (Boateng *et al*., 2024) [13]. Fan palm being a natural and anisotropic material requires a higher safety factor against collapse when designing. Thus, Kankam and Odum-Ewuakye (2001) [23] and Jimoh and Adetifa (1993) [20] suggested a factor of safety of 2 to 3 using babadua and fan palm respectively. These factors of safety are to provide adequate margin of safety measures to avoid abrupt collapse in buildings. Mansal *et al*. (2024) [28, 29] investigated the flexural behaviour of beams reinforced with African fan palm and recommended a factor of safety of 2.5 drawn from studies of Kankam and Odum-Ewuakye (2001) [23] and Jimoh and Adetifa (1993) [20].

2. Experimental Programme

2.1 Specimen Details

A total of fourteen simply supported two-way slabs were cast comprising two sets of slabs of thicknesses 90mm and 100mm and width of 1200mm as described in Table 1. Out of the 14 slabs, 12 were reinforced with the African fan palm bars in both directions, and slabs 7 and 14 reinforced with steel bars. The tensile ratio and the concrete compressive strength as well as the concrete tensile strength were the main test parameters. The skeletal framework of all fan palm reinforced slabs was constructed as illustrated in figure 1 and provided with 12mm concrete cover.

(a) Skeletal framework (b) Fan palm reinforced concrete slab

Fig 1: Details of slab specimen preparation and concreting

Table 1: Description of two-way slabs

Two-way slabs ID	Slab cross section (B x D) (mm)	% Tension rebars	Concrete compressive strength (N/mm²)	Concrete tensile strength (N/mm²)
TWS1	90 x 1200	3.05	15.34	1.83
TWS2	90 x 1200	3.05	15.34	1.83
TWS3	90 x 1200	2.51	15.34	1.83
TWS4	90 x 1200	2.29	22.37	2.22
TWS5	90 x 1200	1.47	22.37	2.22
TWS6	90 x 1200	2.06	22.37	2.22
TWS7*	90 x 1200	0.50	15.34	1.83
TWS8	100 x 1200	3.50	22.37	2.22
TWS9	100 x 1200	3.50	22.37	2.22
TWS10	100 x 1200	1.60	22.37	2.22
TWS11	100 x 1200	1.87	15.34	1.83
TWS12	100 x 1200	3.08	15.34	1.83
TWS13	100 x 1200	3.33	15.34	1.83
TWS14*	100 x 1200	0.64	22.37	2.22

Key: * Steel reinforced two-way concrete slabs.

2.2 Materials
Two concrete strengths of 1:2:4 and 1:1.5:3 were used in accordance with IS 456:2000. Steel reinforcing bars and matured African fan palm bars were converted to sizes of varying percentage tensile ratios and used in the study. Concrete cubes of 150mm x 150 x 150mm and concrete cylinders of 150mm x 300mm were tested at 28-day age to give average compressive strength and splitting tensile strength of 15.34N/mm^2 and 22.37N/mm^2, and 1.83N/mm^2 and 2.22N/mm^2 for ratios of 1:2:4 and 1:1.5:3 respectively. These tests were done in accordance with ASTM C39. The averages of the compressive strengths and split tensile strengths were used for calculations in the theoretical analysis.

2.3 Experimental Setup: The slabs were subjected to flexural loading using a hydraulic jack with a loading cell that was manually operated. The slabs were supported on all four edges and with the aid of a digital dial gauge device placed centrally underneath the slab to measure deflection at every 2kN reading from the hydraulic jack. Assessments of crack patterns, failure modes and ultimate failure loads were recorded to ascertain flexural deformation and hence determine whether the slabs were under-reinforced or over-reinforced. Twelve slabs were loaded monotonically to failure whilst the remaining two were subjected to 10 cycles of loading. The experimental test set-up is illustrated in figure 2. The slabs had an effective span (L_o) of 1050mm and 75mm gap between support and the edge of the slab.

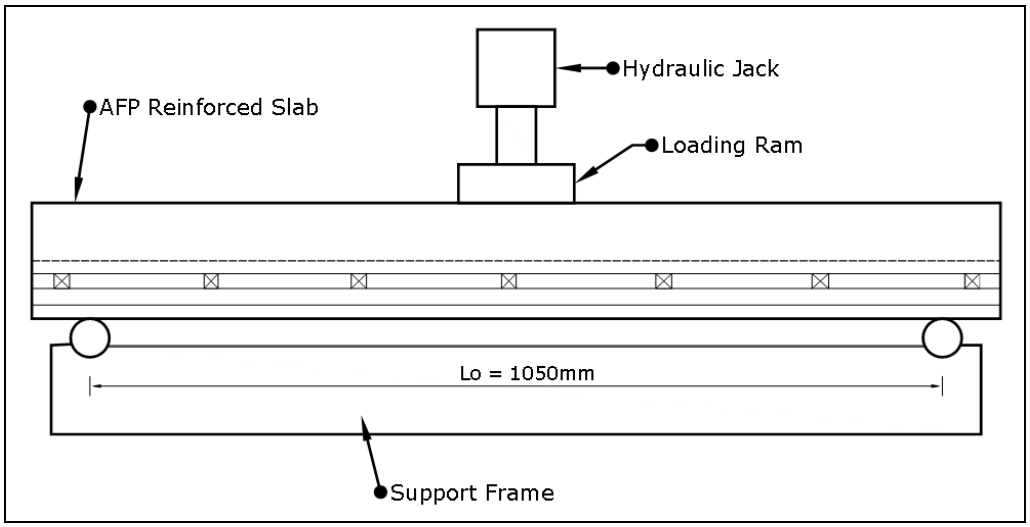

Fig 2: Schematic diagram of the loading set-up.

3. Theoretical Analysis
3.1 Flexural Theory of the Two-Way Slabs
3.1.1 Splitting tensile strength
The split tensile strength of the plain concrete cylinder of diameter 150mm and a length of 300mm was derived from the average applied load based on the 28 days maturity as in equation 1:

$$f_{tc} = \frac{2P}{\pi LD} \quad (1)$$

Where, f_{tc} = the modulus of rupture of the concrete cylinder, P = ultimate applied load and L and D represent both the length and diameter of the cylinder. Based on the two concrete strengths used, the average split tensile strengths of 1:2:4 and 1:1.5:3 were found to be 1.83N/mm^2 and 2.22N/mm^2 respectively.

3.2.1 Cracking Moment
Using the splitting tensile strength, the cracking moment of a two-way fan palm reinforced concrete slab is obtained from the expression as in equation 2:

$$M_{cr} = \frac{f_{tc} b h^2}{6} \quad (2)$$

Where: M_{cr} = cracking moment, b = width of the concrete slab, h = overall thickness of the slab.

3.2.2 Theoretical cracking load: The theoretical cracking load for a simply supported two-way slab centrally loaded is given as in equations 3(a) or 3(b):

$$P_{cr} = \frac{8M_{cr}}{L} \text{ for diagonal cracking load} \quad (3a)$$

$$P_{cr} = \frac{2\pi M_{cr}}{L} \text{ for a circular cracking load} \quad (3b)$$

The least of the cracking load in equations 3(a) and (b) above was used as the theoretical cracking load.

3.3 Theoretical failure loads
The theoretical failure loads of a two-way fan palm reinforced concrete slab simply supported on all four edges and loaded centrally, is based on three assumptions:
1. Fan palm bars failing first or;
2. Concrete crushing or;
3. Punching shear.

3.3.1 Theoretical failure load on the assumption that the fan palm bars fail first
The moment of resistance of fan palm reinforced concrete

slab with a factor of safety of 2.5, assuming that the tension bars fail first is derived as in equation 4:

$$M_{rs} = 0.4 f_{yp} A_{sp}\, x\, 0.775d \quad (4)$$

where: M_{rs} = moment of resistance of fan palm in tension, f_{yp} = average tensile strength of the fan palm, d = effective depth of beam, A_{sp} = area of fan palm reinforcement in the tension zone.
Therefore, the failure load due to diagonal or circular mode is given as in equation 5 (a) and (b):

$$P_{ult} = \frac{8M_{cr}}{L} \text{ for diagonal cracking load} \quad (5a)$$

$$P_{ult} = \frac{2\pi M_{cr}}{L} \text{ for a circular cracking load} \quad (5b)$$

3.3.2 Theoretical failure load on the assumption that the concrete crushes first

The moment resistance of the fan palm reinforced concrete two-way slab, simply supported and centrally loaded on the assumption that the concrete crushes first in compression is derived from equation 6:

$$M_{rs} = 0.156 f_{cu}\, bd^2 \quad (6)$$

where: M_{rs} = moment of resistance based on failure in compression, f_{cu} = compressive strength of concrete, d = effective depth and b = width of the slab.
The failure load due to concrete crushing through diagonal or circular mode is computed as in equation 5(a) and 5(b) above.

3.3.3 Theoretical failure load on the assumption that punching shear failure occurs first

The British Code of Practice BS 8110 estimated that the theoretical punching shear strength is comprised of the concrete section and a total of the concrete section plus the tension reinforcement. Hence, the critical section is derived from equation 7 (Kankam and Odum-Ewuakye, 2006) [24]. Thus, for a loading hydraulic jack base of 127mm diameter, the length of the critical perimeter from the boundary of the loaded area is given in equation 7:

$$L = 2\pi\left(1.5h + \frac{127}{2}\right) \quad (7)$$

where L = the length of the critical perimeter and h = overall slab thickness. The value of length of the perimeter obtained in the above equation is used as the effective width of the slab (b).
After determining the critical length from equation 7, the ultimate shear strength (V_u) is computed as in equation 8:

$$V_u = \upsilon_c bd \quad (8)$$

where: V_u = ultimate shear strength, υ_c = concrete shear strength, b = the perimeter of the punching zone given by equation 7 and d = the lesser effective depth thickness of the slab.

The concrete shear strength (υ_c) is computed as in equation 9, obtained from BS 8110-1-1997 (Table 3.8, note 2).

$$\upsilon_c = 0.79\{100As/(b_v d)\}^{1/3}(400/d)^{1/4} / \gamma_m \quad (9)$$

where: A_s = area of fan palm reinforcement in the tension zone, b_v = slab width, d = the effective thickness of the slab in the lesser direction and γ_m = factor of safety of fan palm as reported by Mansal *et al*. (2024) [28, 29]. For concrete strength (f_{cu}) greater or less than 25 N/mm^2, the code recommends the value of the concrete shear strength (υ_c) to be interpolated in accordance to BS 8110-1:1997.
Using equation 8, the shear failure load (P_{ult}) is computed. The consideration of the theoretical failure loads based on the three assumptions are repeated in the two orthogonal directions. The direction of the lower effective depth of the slab is selected to govern. The minimum failure load from the three assumptions also governs the slab failure load.

4. Discussions of Test Results

4.1 Load-deflection behaviour of slabs under monotonic and cyclic loads

The relationships of the applied load and mid-span deflection are presented in figure 3 for monotonic loading and figure 4 for cyclic loading. Out of the fourteen two-way slabs, TWS8 and TWS9 were the only slabs that were subjected to 10 cycles of loading. At the increase of each cycle load, more cracks were formed and continued to widen up prior to failure. Despite repeated loading and unloading of the slabs, it was observed that the slabs lost minimal stiffness and were able to trace their paths to final ultimate failure load of 40kN (Adom-Asamoah and Kankam, 2008) [2]. Curves obtained from the fan palm reinforced concrete slabs are linearly elastic. During initial loading of the slabs, cracks were noticed which continued to widen depending on the tensile ratio of fan palm reinforcements in the slabs as well as the thickness of the slabs. The post-crack loads exhibited non-linearity of the curves with slabs continuing to reduce in stiffness up to failure. It was observed that TWS 5 with 1.47% tensile ratio, registered the lowest deflection of 13.28mm compared to TWS 11 with the largest deflection of 25mm and a tensile ratio of 1.87%. The steel reinforced concrete slabs (TWS7 and TWS14) deformed in similar manner with almost the same deflection values of 19.24mm and 18.48mm respectively. Failure loads of TWS8 and TWS9 produced maximum deflections of 18.42mm and 22.43mm respectively. Slabs of 90mm thickness produced an average maximum deflection of 20.17mm compared to the 100mm thick slabs with an average maximum deflection of 22.41mm.

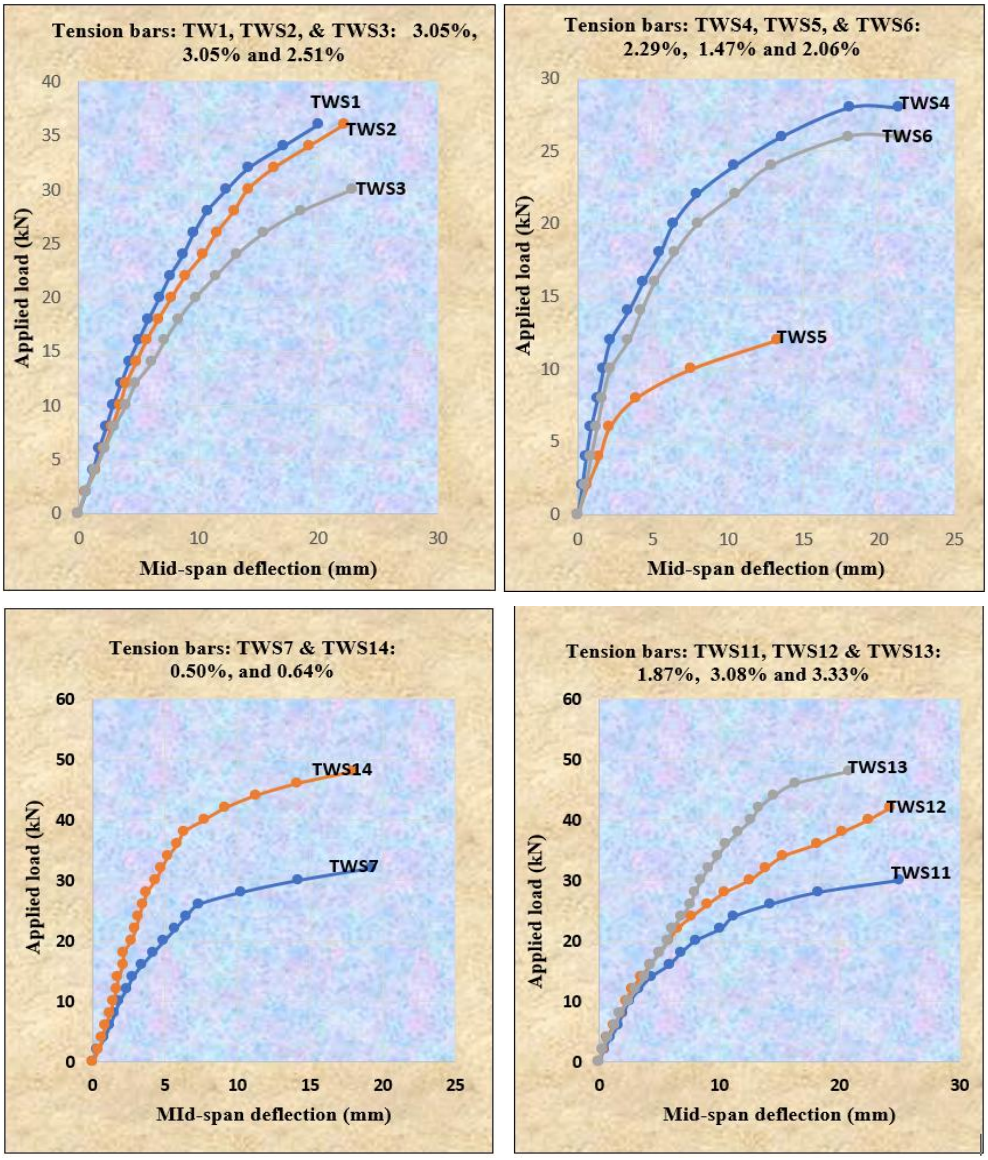

Fig 3: Deflection curves of monotonic loaded two-way slabs

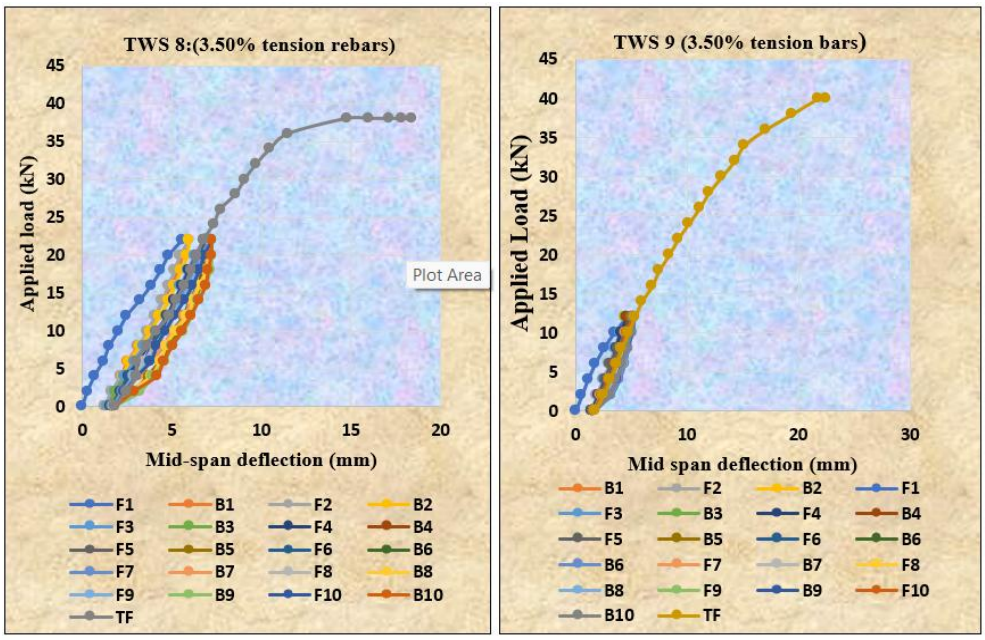

Fig 4: Deflection curves of cyclic loaded two-way slabs

4.2 Cracking Loads

The cyclic loaded slabs formed hysteresis loop and sustained the same theoretical cracking load (P'_{cr}) of 23.28kN (cast from the same concrete strength and the same slab thickness) compared with their experimental cracking loads (P_{cr}) of 12.00kN before propagating to final failure. The cracking load results are based on the compressive concrete strength of 15.34N/mm^2 and 22.37N/mm^2 as well as varying tensile reinforcing bars.

Furthermore, the experimental cracking loads (P_{cr}) of the 90mm thick slabs averaged 0.34 P_{ult} (experimental failure loads) and 0.53 P'_{cr} (theoretical cracking loads), compared to the 100mm thick slabs that showed 0.31 P_{ult} and 0.54 P'_{cr}. On the other hand, the steel reinforced slab TWS7 showed a ratio of experimental cracking loads (P_{cr}) to experimental failure load (P_{ult}) of 0.39, while the experimental cracking loads (P_{cr}) averaged 0.81theoretical cracking loads (P'_{cr}) for the 90mm slabs; and for TWS14, the ratios are 0.31 P_{cr}/P_{ult}, and 0.54 P_{cr}/P'_{cr} for the 100mm slabs. Specimen TWS5 produced the least experimental cracking load of 6kN mainly due to the lowest fan palm tensile reinforcing bars of 1.47% compared to TWS8 and TWS9 with the highest tensile ratio of 3.50%. Specimens TWS8, TWS9, TWS10 and TWS14 were noticed to have the largest theoretical cracking loads of 23.28kN attributed to the concrete compressive strength of 22.37N/mm^2.

Table 2: Experimental and theoretical failure loads of two-way slab

				Theoretical failure load P'ult (kN): Based on										
		Experimental		X - Direction			Y - Direction orthogonal to X							
Two-way slab ID	P'cr	Pcr	Pult (kN)	Tension bars (Fan palm/steel)	Concrete crushing	P S	Tension bars (Fan palm/steel)	Concrete crushing	P S	P'ult/ P'cr	Pult/ Pcr	Pcr / P'cr	Pcr/ Pult	Pult/ P'ult
TWS1	15.50	10.00	36.00	31.48	73.66	52.38	24.29*	43.86	46.47	1.57	3.60	0.65	0.28	1.48
TWS2	15.50	10.00	36.00	31.48	73.66	52.38	24.29*	43.86	46.47	1.57	3.60	0.65	0.28	1.48
TWS3	15.50	8.00	30.00	27.27	73.66	48.02	20.76*	47.15	43.30	1.34	3.75	0.52	0.27	1.45
TWS4	18.85	10.00	28.00	23.58	107.41	53.26	18.19*	68.76	48.19	1.00	2.80	0.53	0.36	1.48
TWS5	18.85	6.00	12.00	14.30	101.37	44.95	10.95*	59.30	40.21	0.58	2.00	0.32	0.50	1.10
TWS6	18.85	10.00	26.00	20.05	101.37	50.89	14.89*	59.30	44.75	0.79	2.60	0.53	0.38	1.75
Avg.	17.18	9.00	28.00	24.69	88.52	50.31	19.02*	53.71	44.90	1.14	3.06	0.53	0.34	1.46
TWS7	15.50	12.50	32.00	25.73	63.55	27.56	21.78*	45.48	54.19	1.41	2.56	0.81	0.39	1.47
TWS8	23.28	12.00	40.00	47.22	134.36	70.84	37.76*	89.77	65.26	1.62	3.33	0.52	0.30	1.06
TWS9	23.28	12.00	40.00	47.22	134.36	70.84	37.76*	89.77	65.26	1.62	3.33	0.52	0.30	1.06
TWS10	23.28	10.00	26.00	21.60	140.34	54.74	17.24*	89.77	50.66	0.74	2.60	0.43	0.38	1.51
TWS11	19.15	10.00	30.00	25.20	96.23	51.52	20.17*	61.58	46.37	1.05	3.00	0.52	0.33	1.49
TWS12	19.15	12.00	42.00	39.44	91.51	59.65	31.36*	57.81	54.08	1.64	3.50	0.63	0.29	1.34
TWS13	19.15	12.00	48.00	42.73	91.51	60.70	34.00*	57.81	54.90	1.78	4.00	0.63	0.25	1.41
Avg.	21.22	11.33	37.67	37.24	114.72	61.38	29.72	74.42	56.09	1.41	3.29	0.54	0.31	1.31
TWS14	23.28	18.00	48.00	42.19	120.11	83.40	35.37*	84.33	77.36	1.52	2.67	0.88	0.38	1.36

Key: *Governing failure; P S = Punching shear;
P_{cr} = Experimental cracking load;
P'_{cr} =Theoretical cracking load;
P_{ult} = Experimental failure load; and P'_{ult} = Theoretical failure load
TWS7 and TWS 14 (control slabs)
Avg. = Averages, exclude control slabs

4.3 Crack Pattern and Mode of Failure

Figure 5 shows the cracking patterns and mode of failure observed at failure of the two-way slabs. Generally, slab failure could result in a combination of modes with the least being adopted as the governing factor. In this experimental test, flexural shear diagonal mode of failure was observed in all the slabs. Loads were applied centrally on the slabs using a hydraulic jack of 200kN capacity. The collapse of the slabs was dictated by the yielding of the fan palm bars, mainly due to the lower tensile ratios, concrete strength and the depth of the concrete slabs. Specimen TWS4 exhibited the widest maximum crack of 10mm. The maximum crack widths of the fan palm reinforced slabs averaged 4.83% for the 90mm slabs and 4.17% for the 100mm slabs. On the other hand, the 100mm slabs had an increase deflection of 10% over the 90mm thick slabs. The increase is attributed to the tensile ratio of fan palm and the strength of the concrete used. Specimens TWS8 and TWS9 at collapse, demonstrated crack propagation radiating from the bottom of the panels with maximum crack width of 2mm each at experimental failure load of 40kN. These two slabs were reinforced with the largest fan palm tensile ratio of 3.50%, thus exhibiting the smallest crack widths. Alternatively, the slabs with the least fan palm bar dimension were seen to have the largest maximum crack width at failure (TWS3, TWS4, TWS5 and TWS11). TWS14 reinforced with steel had resulting stresses built around the loading area thus producing a weaken deformation at collapse load of 48kN recording a 3mm maximum crack width.

Diagonal yield failure mode TWS9 Diagonal yield failure mode TWS8

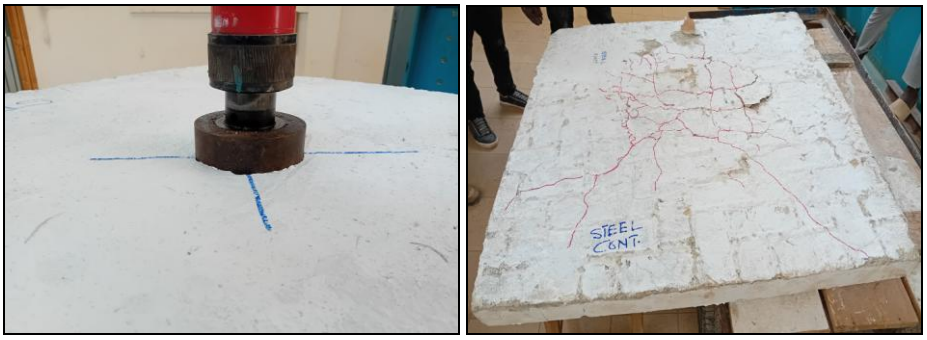

TWS14 at failure showing cracks radiating to the edges and corners of the slab

Fig 5: Modes of failures of two-way slabs

Table 3: Crack Pattern and Mode of Failure of Two-way Slabs

TWS ID	Max. deflection (mm)	Max. crack width (mm)	Failure mode
TWS1	20.05	2	Flexural-shear
TWS2	22.20	4	Flexural-shear
TWS3	22.86	6	Flexural-shear
TWS4	21.35	10	Flexural-shear
TWS5	13.28	4	Flexural-shear
TWS6	21.30	3	Flexural-shear
Avg.	20.17	4.83	
TWS7	19.24	4	Flexural-shear
TWS8	18.42	2	Flexural-shear
TWS9	22.43	2	Flexural-shear
TWS10	23.63	5	Flexural-shear
TWS11	25.00	6	Flexural-shear
TWS12	24.20	7	Flexural-shear
TWS13	20.77	3	Flexural-shear
Avg.	22.41	4.17	
TWS14	18.48	3	Flexural-shear

4.4 Failure Loads

A detail summary of the experimental and theoretical failure loads is presented in Table 2. All specimens failed by the yielding of the tensile fan palm/steel bars around the central bottom area of the slabs. This was also predicted by the theoretical analysis indicating failure due to yielding of the fan palm bars. Moreover, the tensile fan palm reinforcement ratios were less than the limit range of steel stipulated in the BS 8110 and the IS 456:2000 to initiate over reinforced slabs. Therefore, since the fan palm is a heterogeneous material, it is only logical for the tensile reinforcement ratio to exceed the 4% of that of steel to initiate over reinforcement. The steel reinforced slabs (TWS7 and TWS14) with 0.50% and 0.64% tensile ratios, showed experimental load capacities of 32kN and 48kN and theoretical failure loads of 21.78kN and 35.37kN respectively. The experimental load capacities of the steel reinforced slabs were found to be 1.50 times higher than the theoretical failure capacities. Similarly, specimens TWS8, TWS9 which were tested cyclically and made from the same concrete strength and the same slab thickness, sustained failure loads of 40kN. The high tensile ratio and concrete strength of these two slabs, contributed to their additional load carrying capacities as supported by Janus *et al*. (2018) [19]. The experimental and theoretical failure loads of the 90mm fan palm reinforced concrete slabs (TWS1-TWS6) averaged 28kN and 19.02kN respectively. Similarly, the 100mm thick slabs (TWS8 to TWS13) recorded average experimental and theoretical failure loads of 37.67kN and 29.72kN respectively. The ratio of the average experimental failure loads (P_{ult}) to theoretical failure loads (P'_{ult}) of all fan palm reinforced slabs TWS1-TWS6 to TWS8 -TWS13

ranged from 1.46 to 1.31 compared to the steel reinforced slabs that varied from 1.47 to 1.36. This is a good indicator of the margin of safety exhibited by the fan palm and steel bars respectively. The differences in these ratios for different fan palm reinforced slabs could be due to the varying reinforcing ratios and strength of the concrete. Furthermore, the experimental failure loads of the fan palm reinforced slabs with thicknesses of 90mm and 100mm (TWS1 – TWS6 and TWS8 – TWS13), show average increase of 306% and 329% respectively, over the experimental cracking loads. The control slabs (TWS7 and TWS14) had experimental failure loads that represented an increase of 256% for the 90mm slabs and 267% for the 100mm slabs over experimental cracking loads. These increases in strength of the slabs beyond cracking are evidence of the contribution of both fan palm and steel bars in the tensile region of the slabs.

5. Determination of Fan Palm Tensile Ratio (ρ) in Reinforced Slabs

Previous studies conducted by Jimoh and Adetifa (1993) [20] on the behaviour of fan-palm reinforced concrete one-way slabs subjected to flexural loading, suggested a 4% maximum limit of fan palm reinforcement in order to avoid compression failure. While this may be plausible based on the anisotropic nature of the fan palm, the tensile strength ratio of steel reinforcement (mild and high yield strength deformed bars) of slabs according to BS 8110 and IS 456:2000 reported a maximum limit percentage tensile ratio of 4%. Similar studies by Archila *et al*. (2018) [6] compared the design strengths of steel and bamboo, based on the nominal tensile capacity and proposed the use of additional bamboo in the tension area. Pam *et al*. (2001) [31] investigated the flexural strength and ductility of reinforced normal and high-strength concrete beams. The authors reported that the use of minimum tensile reinforcement in concrete members irrespective of concrete grade, allow tension cracks to form with large deflection prior to collapse. Similar test was conducted by the authors on beams which were over reinforced with results showing few tension cracks and abrupt and brittle failure. The ACI code (2015) also underscores the dangers of over-reinforcements in reinforced concrete structural elements so as to evade brittle failure with catastrophic and sudden collapse. The African fan palm bars is known to exhibit similar behaviour to the Glass Fiber Polymer Bars (GFP) and bamboo with a brittle failure when over reinforced. Furthermore, these reinforcing materials are found to exhibit low modulus of elasticity. Correal (2016) [15] examined the tensile modulus of *Guadua angustifolia* bamboo and reported a 20GPa, representing a 10% to that of steel. Similar studies from Asibe *et al*. (2013) [7]; Gbaguidi-Aisse *et al*. (2011) [16] and Mansal *et al*. (2024) [28, 29], all highlighted low modulus of elasticity of the African fan palm as 17.13kN/mm^2, 17.20kN/mm^2 and 20kN/mm^2 respectively. Hence, under-reinforced design ensures reserve capacity prior to collapse (Archila *et al*., 2018) [6]. Based on the above, this study compared the BS 8110 Part 01:1997 and IS 456:2000 tensile design limit ratios of steel. The two standards show minimal variation limits of the tensile strength. Hence, the behaviour of the African fan palm was examined, and a factor of safety of 2.5 and an average tensile strength of 94.67N/mm^2 (Mansal *et al*., 2024) [28, 29] were used to derive the tensile limits of mild steel from equations 6 (a) and 7 (a) (IS 456:2000) to give equations 6(b) and 7(b):

$$\rho_{min.} = 0.15bD \quad 6(a)$$

$$\rho_{max} = 4bD \quad 7(a)$$

$$\rho_{min.} = 0.15bD + 0.4(0.15bD) \quad 6(b)$$

$$\rho_{max} = 4bD + 0.4(4bD) \quad 7(b)$$

where ρ_{min} = minimum tensile ratio, ρ_{max} = maximum tensile ratio, b = width of the slab and D = effective depth of the slab.

Therefore, the limiting values of the fan palm structural members that govern sufficient tension reinforcement for fan palm with a factor of safety of 2.5 fall within 0.21% minimum to 5.60% maximum tensile ratios. These limiting values were used as well as observations from the experimental results, to determine the adequacy of tensile ratios for all slabs. It was observed that the tensile ratios of all the slabs fell below the maximum limit of 5.60%, indicating that the slabs were under-reinforced.

6. Conclusions and Recommendations

The monotonic and cyclic loading tests were carried out to investigate the behaviour of fan palm reinforced two-way slabs with varying tensile ratios. Experimental and theoretical analysis were used to examine the load-deflection properties, mode of failure, crack pattern and ultimate failure loads of the slabs to evaluate suitability of fan palm as reinforcing material. Based on the experimental investigation, the following observations and conclusions are drawn:

1. The African fan palm is a suitable alternative material to steel reinforcement for use in concrete elements despite its low Young's modulus of elasticity, provided a desired factor of safety of 2.5 is used in the ultimate limit state during the design phase.
2. All the slabs experienced flexural-shear failure, through the fan palm bars failing first.
3. It was observed that the steel reinforced slabs demonstrated higher experimental cracking loads compared to the fan palm reinforced slabs.
4. Like GFRP bars, the mechanical tensile strength of the African fan palm bars exhibited linear elastic curve with brittle failure.
5. It was observed that the ultimate load carrying capacity of the slabs, were influenced by the increase in tensile ratio as well as the compressive strength of the concrete.
6. Based on the results of the study, proposed simple equations are provided for the calculations of the limits of tensile reinforcement of the African fan palm ranging from 0.21% - 5.60%. These limits were compared with the experimental failure loads, thus indicating that all slabs were under reinforced.

7. Acknowledgements

The authors acknowledge the support provided by the Department of Civil Engineering of the Kwame Nkrumah University of Science and Technology (KNUST), Kumasi, Ghana.

8. Conflicts of Interest

The authors declare no conflict of interest.

9. References

1. Adedeji RO. Determination of the utilization potentials of wood of *Borassus aethiopum* Mart through its strength properties. Journal of the Indian Academy of Wood Science. 2020; 17:119–127. doi:10.1007/s13196-020-00263-z.
2. Adom-Asamoah M, Kankam CK. Behaviour of reinforced concrete two-way slabs using steel bars milled from scrap metals. Materials and Design. 2008;29(6):1125–1130. doi:10.1016/j.matdes.2007.06.001.
3. Adom-Asamoah M, Banahene JO, Obeng JB. Bamboo-reinforced self-compacting concrete beams for sustainable construction in rural areas. Structural Concrete. 2017;18(2):317–327. doi:10.1002/suco.201600205.
4. Agyarko K, Kannuba SJ, Russel B, Menkah KT, Antuong IS. Views of preventing *Borassus aethiopum* from extinction among four communities in Ghana. Journal of Natural Sciences Research. 2014;4(2):1–7.
5. American Concrete Institute (ACI). ACI 440.1R-15 Guide for the Design and Construction of Structural Concrete Reinforced with Fiber-Reinforced Polymer (FRP) Bars. Farmington Hills (MI): American Concrete Institute; c2015.
6. Archila H, Kaminski S, Trujillo D, Escamilla EZ, Harries KA. Bamboo reinforced concrete: a critical review. Materials and Structures. 2018; 51:102. doi:10.1617/s11527-018-1228-6.
7. Asibe AAO, Frimpong-Mensah K, Darkwa NA. Assessment of the effect of density on mechanical properties variations of *Borassus aethiopum*. Archives of Applied Science Research. 2013;5(6):6–19.
8. ASTM International. ASTM C39/C39M: Standard Test Method for Compressive Strength of Cylindrical Concrete Specimens. West Conshohocken (PA): ASTM International; c2001.
9. Audu MT, Oseni OW. First crack and yield load of fan palm reinforced concrete slabs. International Journal of Science and Research. 2015;4(11):1404–1409.
10. Audu MT, Raheem AA. Flexural behaviour of fan palm reinforced concrete slabs. Annals of Faculty Engineering Hunedoara – International Journal of Engineering. 2017;15(1):47–53.
11. Ayarkwa J. Potential for utilisation of *Borassus aethiopum* (fan palm) in construction in Ghana. Forestry Research Institute of Ghana; c2007.
12. Forestry Research Institute of Ghana. Demography of a savanna palm tree: prediction from comprehensive spatial pattern analysis. Ecology. 1999;80(6):1987–2005.
13. Boateng GO, Kankam CK, Mansal EC, Afrifa RO, Kwarteng F, Ohene-Coffie F, Kpo SAK. Evaluating the mechanical properties of fiberglass-reinforced polymer bar. Journal of Engineering Research and Reports. 2024;26(7):150–60. doi:10.9734/jerr/2024/v26i71200.
14. British Standards Institution. BS 8110-1: Structural Use of Concrete – Part 1: Code of Practice for Design and Construction. London: British Standards Institution; c1997.
15. Correal JF. Bamboo design and construction. In: Harries K, Sharma B, editors. Nonconventional and Vernacular Construction Materials: Characterisation, Properties and Applications. Cambridge: Woodhead Publishing; c2016. p. 365–400.
16. Gbaguidi-Asse LG, Gbaguidi VS, Gibigaye M, Amadji TA, Agossou YD, Soclo P, *et al*. Étude de la possibilité d'utilisation du Borassus comme armature dans les éléments en béton: cas des poutres. Annales des Sciences Agronomiques. 2011;15(1):67–68.
17. Gbesso F, Adjatin A, Dansi A, Akoegninou A. Aphrodisiac properties of hypocotyls extract of *Borassus aethiopum* Mart. (Arecaceae) collected in Central Benin Republic. International Journal of Current Microbiology and Applied Sciences. 2016;5(4):802–814.
18. International Centre for Research in Agroforestry (ICRAF). A Selection of Useful Trees and Shrubs for Kenya: Notes on Their Identification, Propagation and Management. Nairobi: ICRAF; c1992.
19. Janus O, Girgle F, Kostiha V, Stepanek P. Effect of surface treatment and test configuration on bond behaviour of GFRP rebars. In: Proceedings of the 9th International Conference on Fibre-Reinforced Polymer (FRP) Composites in Civil Engineering; c2018 Jul 17–19; Paris, France.
20. Jimoh AA, Adetifa OA. Behaviour of fan palm reinforced concrete one-way slabs subjected to flexural loading. In: Proceedings of the Structural Engineering Analysis and Modelling Conference; c1993 Jul 27–29; Accra, Ghana.
21. Joshua A. Potential for utilisation of *Borassus aethiopum* (fan palm) for construction in Ghana. Kumasi: Forestry Research Institute of Ghana; c1997.
22. Kankam CK. Raffia palm-reinforced concrete beams. Materials and Structures. 1997;30(6):313–316. doi:10.1007/BF02486356.
23. Kankam CK, Odum-Ewuakye B. Flexural behaviour of babadua reinforced one-way slabs subjected to third-point loading. Construction and Building Materials. 2001;15(1):27–33.
24. Kankam CK, Odum-Ewuakye B. Babadua reinforced concrete two-way slabs subjected to concentrated loading. Construction and Building Materials. 2006;20(4):279–285.
25. Kankam JA, Ben-George M, Perry SH. Bamboo-reinforced beams subjected to third-point loading. ACI Structural Journal. 1988;85(1):61–67.
26. Kone O, Otieno Koteng D, Matallah M, Kabubo CK. Mechanical characteristics of Kenyan *Borassus aethiopum* Mart timber as reinforcement for concrete. International Journal of Civil Engineering. 2021;8(11):7–12.
27. Kumar P, Gautam P, Kaur S, Chaudhary M, Afreen A, Mehta T. Bamboo as reinforcement in structural concrete. Materials Today: Proceedings. 2021;46(4):1701–1707. doi:10.1016/j.matpr.2021.04.342.
28. Mansal EC, Kankam CK, Banahene JO, Afrifa RO. Experimental investigation on the mechanical properties of African fan palm (*Borassus aethiopum*).

IOSR Journal of Mechanical and Civil Engineering. 2024;21(4):8–17. doi:10.9790/1684-2104020817.
29. Mansal EC, Kankam CK, Biney E, Akortia V, Babamu A. Flexural behaviour and environmental impact of African fan palm reinforced concrete beams under symmetrical loading conditions. Journal of Scientific Research and Reports. 2024; XX:1–10.
30. Michon L, Adeoti K, Koffi K, Ewedje EE, Stauffer F. Notes on *Borassus aethiopum* Mart.: a multi-purpose palm in Togo and Benin. Journal of the International Palm Society. 2018;62(2):57–64.
31. Pam HJ, Kwan AKH, Islam MS. Flexural strength and ductility of reinforced normal-and high-strength concrete beams. Proceedings of the Institution of Civil Engineers – Structures and Buildings. 2001;146(4):381–389.
32. Parveen, Sharma A. Structural behaviour of jute fiber reinforced concrete beams under bending. International Journal of Engineering Research and Applications. 2013;3(3):108–110.
33. Samah OD, Amey KB, Neglo K. Determination of mechanical characteristics and reaction to fire of "Ronier" (*Borassus aethiopum* Mart) of Togo. African Journal of Environmental Science and Technology. 2015;9(2):80–85. doi:10.5897/AJEST2014.1767.
34. Sohounhloue AYJ, Gbaguidi-Aisse GL, Houehanou CE, Foudjet AE. *Borassus aethiopum* of Benin used as vegetable reinforcement in concrete: characterization of the overlapping zone; c2018.
35. IS 456:2000: Plain and Reinforced Concrete – Code of Practice of India.